Nanoscale Advances

ROYAL SOCIETY OF CHEMISTRY

MINIREVIEW

View Article Online
View Journal | View Issue

Cite this: *Nanoscale Adv.*, 2022, **4**, 3504

Recent advances in redox-responsive nanoparticles for combined cancer therapy

Yanjun Yang[a] and Wen Sun *[ab]

The combination of multiple therapeutic modalities has attracted increasing attention as it can achieve better therapeutic effects through different treatment mechanisms. However, traditional small molecule agents are non-specific to the tumor tissue, which leads to off-target toxic effects for healthy tissues. To solve this problem, a number of stimuli-responsive nanoscale drug-delivery systems have been developed. Among these stimuli, a high concentration of reactive oxygen species (ROS) and glutathione (GSH) are characteristic of the tumor microenvironment (TME), which can distinguish it from normal tissue. In this review, we summarize the redox-responsive nanoparticles (NPs) reported in the past three years classified by different functional groups, including GSH-responsive disulfide, ditelluride, and multivalent metal ions, ROS-responsive thioketal, arylboronic ester, aminoacrylate, and bilirubin as well as GSH/ROS dual-responsive diselenide and dicarbonyl thioethers. The prospects and challenges of redox-responsive NPs are also discussed.

Received 8th April 2022
Accepted 20th July 2022

DOI: 10.1039/d2na00222a

rsc.li/nanoscale-advances

1. Introduction

Despite rapid developments in medicinal and pharmaceutical chemistry, cancer treatment is still a major challenge.[1] Recently, as a new approach for curing cancer, phototherapy has demonstrated promising prospects due to its minimal invasiveness and high specificity.[2–5] However, sole treatment approaches, including chemotherapy or phototherapy, show limitations because of their inherent deficiency and tumor heterogeneity. For instance, chemotherapy can achieve systemic treatment, but always causes damage to normal tissues, making patients suffer from serious adverse reactions.[6–9] In addition, the multidrug resistance (MDR) of tumor cells usually emerges after several courses of chemotherapy.[10] Although phototherapy, including photothermal therapy (PTT) and photodynamic therapy (PDT), is efficient for irradiated tumor tissue, phototherapy is not capable of curing metastatic tumors.[11–15] Therefore, the combination of multiple therapeutic modalities has attracted increasing attention as it can overcome the disadvantages of sole treatment to achieve enhanced therapeutic effects.[16–20] For example, chemotherapy combined with phototherapy is one of the widely used strategies, and reduces

[a]*State Key Laboratory of Fine Chemicals, Dalian University of Technology, Dalian 116024, China. E-mail: sunwen@dlut.edu.cn*
[b]*Ningbo Institute of Dalian University of Technology, Ningbo 315016, China*

Yanjun Yang is currently pursuing a Master's Degree under the supervision of Prof. Wen Sun at the State Key Laboratory of Fine Chemicals, Dalian University of Technology. Her research interest focuses on the design and development of activatable drug and photosensitizer delivery systems for the anticancer treatment.

Wen Sun received his PhD in 2017 from the Max Planck Institute for Polymer Research (Germany). He joined Dalian University of Technology as an associate professor in 2018, where he became a full professor in 2020. His research focuses on developing functional dyes and photoresponsive materials for biomedical applications, including bioimaging, fluorescence diagnosis, and phototherapy. To date, he has authored more than 50 papers in international journals with an H-index of 40. He recently became an associate editor of Frontiers in Chemistry in 2022.

the dosage of agents to minimize the side effects of each treatment modality, while chemoradiotherapy is a therapeutic paradigm of various cancers in clinic. In addition, immunotherapy modulates the autoimmune responses to suppress tumor growth and prevent tumor recurrence in combination with other modalities. However, most therapeutic reagents are non-specific to the tumor tissue, which can lead to serious toxic side effects on normal tissues. Nanoscale drug-delivery systems (DDSs) can passively target tumor sites through the enhanced permeability and retention (EPR) effect.[21–27] NPs co-loaded with anticancer agents with a diameter of 10–200 nm (optimal size selection) tend to accumulate in the tumor tissue, which improves their availability and reduces systemic side effects.[28,29] However, the premature leakage of cargo during blood circulation remains a major problem hindering the therapeutic efficacy.

To further enhance the precise release of anticancer agents, stimuli-responsive NPs have been extensively designed that can be activated by endogenous and exogenous stimuli.[30–35] In general, endogenous stimuli refer to the tumor microenvironment (TME), including weak acid, hypoxia, disordered redox species, and overexpressed enzymes.[36] Numerous studies have focused on TME-responsive NPs for precise drug delivery to achieve excellent treatment effects.[37,38] For example, NPs with pH-sensitive bonds or functional groups enabled precise drug release through bond cleavage or functional group isomerization.[39–43] Hypoxic pathological environments lead to an overexpression of different biological reductases, including nitroreductase (NTR), azoreductase (AZR), and quinone reductase.[44,45] The targeting ability of nanomaterials can be significantly improved by incorporating hypoxia-sensitive groups, such as nitroimidazole (NI) and azobenzene (Azo) derivatives to achieve response to biological reductases.[46,47] Moreover, some overexpressed enzymes, such as aminopeptidase N (APN), matrix metalloproteinases (MMPs), and carbonic anhydrase IX (CAIX), have also been used as the specific stimuli for cancer theranostics.[48–51]

Among the aforementioned stimuli factors, redox species play an important role in the design of TME-responsive NPs.[52–55] Reactive oxygen species (ROS) include non-radical species, including hydrogen peroxide (H_2O_2) and singlet oxygen ($^1O_2$), as well as radical species, such as hydroxyl radicals ($^{\bullet}OH$) and superoxide anion radicals ($O_2^{\bullet-}$). Substantial evidence has shown that cancer cells produce higher concentration of ROS mainly due to mitochondrial dysfunction.[56–59] In another aspect, glutathione (GSH) is a reduced biothiol, which is widespread in living organisms.[60,61] It is worth noting that the concentration of GSH in tumor cells can reach 2–10 mM, which is 7–10 times higher than that in normal tissues.[62,63] Therefore, both ROS and GSH are specific parameters in cancer cells. Moreover, ROS and GSH can react with specific functional groups (Table 1). Specially, thioketal can be oxidized by ROS to yield two thiol fragments and one acetone molecule, while arylboronic ester is oxidized by H_2O_2 and further hydrolyzes to release the phenol and boric acid, and the β-aminoacrylate linkage undergoes fast oxidative degradation, resulting in cleavage of the ester bond.[64–66] Besides, bilirubin (BR) turns from a hydrophilic to hydrophobic group in the presence of

Table 1 Redox-responsive groups and their responsiveness behaviors

Responsive groups	Stimulus	Responsiveness behavior(s)	Therapeutic modalities	Ref.
Disulfide	GSH	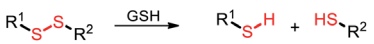	Chemoradiotherapy	83
			PDT, PTT	87
Ditelluride	GSH	Similar to disulfide	Chemotherapy	88
			PDT, PTT, CDT	92
Metal ions	GSH	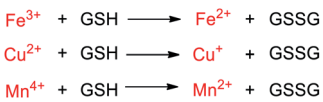	PDT, PTT, CDT	93
			PTT, CDT	94
Thioketal	ROS	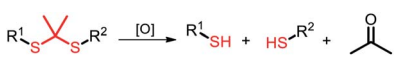	Chemo-PDT	98
			Chemo-PDT	99
Arylboronic ester	H_2O_2	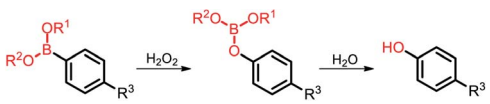	PDT, PTT	102
			Chemoradiotherapy	105
Aminoacrylate	ROS	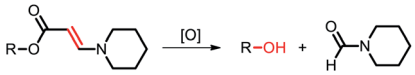	Chemo-PDT	108
Bilirubin	ROS	Change from hydrophilic to hydrophobic	Chemo-photodynamic-immunotherapy	111
			Chemo-immunotherapy	120
Diselenide	ROS/GSH	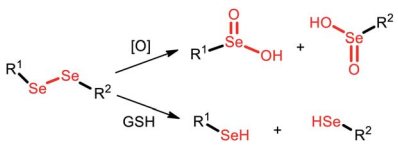	Chemo-photodynamic-immunotherapy	121

ROS.[67] While, disulfide bonds are broken by GSH through disulfide–thiol exchange reaction, ditelluride bonds are similarly cleaved, and high-valent metal ions can also be reduced to low-valent in the presence of GSH.[68,69] Notably, some moieties are sensitive to both ROS and GSH.[54] For example, diselenide can simultaneously react with ROS or GSH to form seleninic acid and selenol units. Therefore, with redox species as the stimulus, a series of smart nanoplatforms based on the responsive moieties have been developed for cancer treatment.[70–75] In this review, we summarized the recent research progress of redox-responsive nanoplatforms for combined cancer therapy. This minireview contains three main parts, in which GSH- (Section 2), ROS- (Section 3), and GSH and ROS dual-responsive NPs (Section 4) are separately summarized. The design strategies of these NPs and their successful applications as nanoplatforms for cancer therapy are discussed in detail. Future developments and challenges in this field are also discussed. The purpose of this minireview is to provide a general overview of the development of redox-responsive NPs for combined cancer therapy, and to stimulate future research studies in this research field.

2. GSH-responsive NPs for combined cancer therapy

Due to the uneven distribution of GSH between tumor cells and extracellular fluid, GSH-responsive moieties as linkers of nanostructured frameworks show promising application in DDSs.[76] Moreover, GSH, as a reducing agent, undergoes redox reactions with some metal-based nanomaterials. The reduced metal ions are further used in tumor diagnosis and therapy, which has been extensively studied.[77–79]

2.1. Disulfide bonds-based GSH-responsive NPs

Disulfide bonds can be cleaved by biothiols, which are the most common moieties applied in designing GSH-responsive NPs.[80–82] Commonly, disulfide bonds are introduced into the polymer chain to connect the prodrug molecules or as a carrier for agent delivery. Amphiphilic polymers self-assemble into nanoscale particles that are enriched at the tumor site through the EPR effect, and the disulfide bonds are broken in the presence of GSH to release the cargoes. For instance, Gan and co-workers[83] designed an amphiphilic polymer with a high disulfide density to self-assemble with a Pt(IV) prodrug. The assemblies exhibited sensitive GSH responsiveness and a high Pt-encapsulation efficiency. Importantly, compared with free cisplatin, the NPs demonstrated the synergistic effects of GSH clearance and mitochondrial damage, easily reversing cisplatin resistance, as well as transporting and releasing more drugs to cisplatin-resistant cells (Hela-CDDP). In addition, Hela-CDDP cells were sensitized to X-ray radiation due to the higher intracellular Pt content of the NPs, which was beneficial for cancer chemoradiotherapy. The results of *in vivo* experiments showed that NPs could effectively accumulate in tumors, resulting in a reduction in the single injection of cisplatin, effectively inhibiting the tumor growth in cisplatin-resistant xenograft models and alleviating the occurrence of serious side effects. The introduction of X-rays further enhanced the anticancer effect of NPs for synergistic chemoradiotherapy (Fig. 1). Luo and co-workers[84] not only linked the chemotherapeutic drug DOX with GSH-responsive disulfide bonds, but also inserted disulfide bonds into the polymer backbone for delivering the photosensitizer chlorine6 (Ce6) inside tumor cells. The disulfide bond-bridged polymeric prodrug showed GSH-triggered dual drug and photosensitizer release for combined chemo-photodynamic therapy.

However, polymer-based redox-responsive prodrugs or pro-photosensitizers have demonstrated some drawbacks, including complex synthetic modifications and a low loading efficiency. In order to solve these problems, carrier-free nanosystems based on the self-assembly of amphiphilic small molecules have been developed.[85,86] Pei and co-workers[87] synthesized amphiphilic small molecules consisting of a hydrophobic photosensitizer and a hydrophilic lactose, which was linked by GSH-responsive disulfide bonds (Fig. 2a). The amphiphilic small molecules enabled the self-assembly into NPs, targeting Hepg-2 cells through the lactose receptor on the

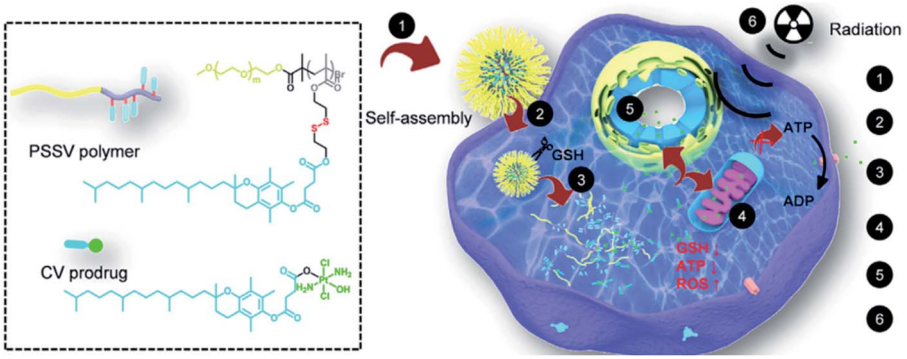

Fig. 1 Chemical structures of the CV prodrug and PSSV polymer and schematic illustration of the mechanism of action of the redox-responsive nanosensitizer in cisplatin-resistant cancer cells.[83] Reproduced with permission from ref. 83. Copyright © 2020, Elsevier Ltd.

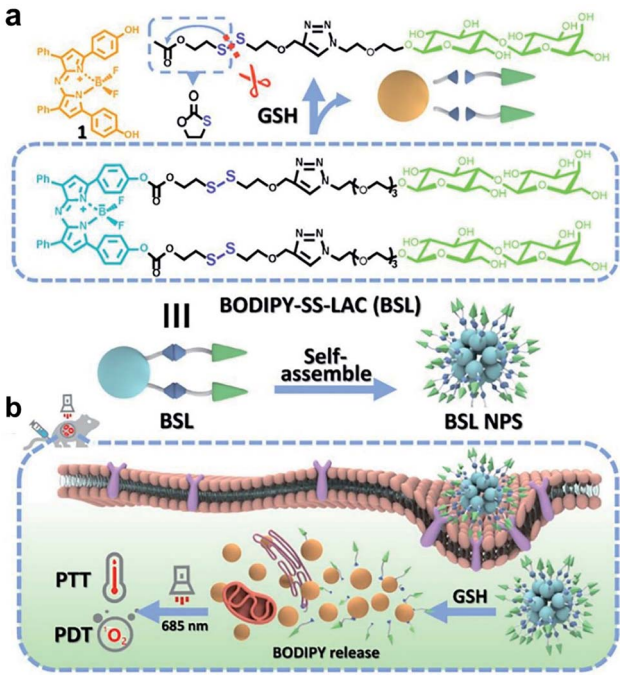

Fig. 2 (a) Chemical structure, self-assembly, and GSH responsiveness of BSL. (b) Schematic representation of BSL NPS for lactose-mediated endocytosis, intracellular BODIPY release triggered by GSH, and DPT with a NIR light of 685 nm wavelength.[87] Reproduced with permission from ref. 87, copyright © 2021, Elsevier Ltd.

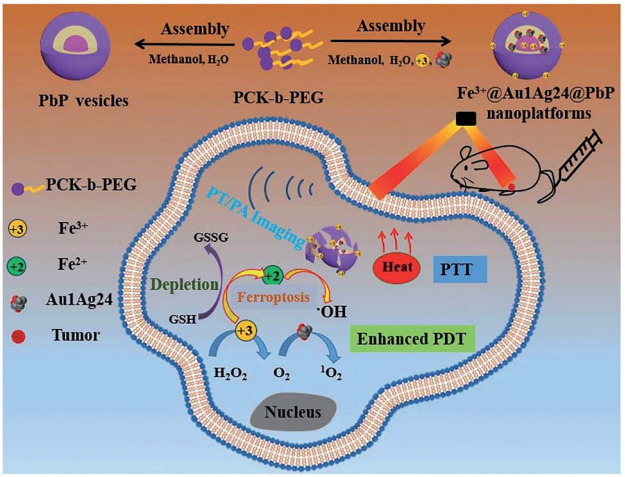

Fig. 4 Schematic illustration of the formation of the Fe^{3+}@Au_1-Ag_{24}@PbP nanoplatform and its imaging-guided synergistic anticancer therapy.[92] Reproduced with permission from ref. 92. Copyright © 2021, The Royal Society of Chemistry.

cell membrane and the responsiveness to GSH. The NPs released the phototherapeutic agent BODIPY due to the cleavage of disulfide bonds by overexpressed GSH at the tumor site; thereby realizing PTT and PDT under the irradiation of a 685 nm laser (Fig. 2b). The carrier-free multifunctional NPSs exhibited good biocompatibility, enhanced enrichment in the tumor, and an excellent anticancer effect.

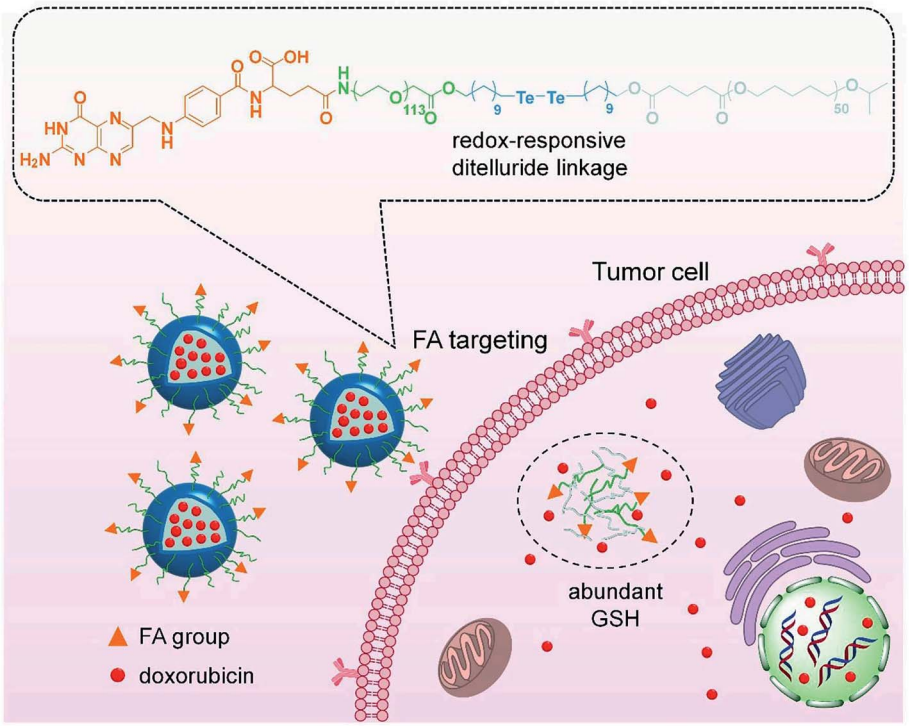

Fig. 3 Schematic of targeted drug delivery and GSH-responsive drug release.[88] Reproduced with permission from ref. 88, copyright © 2020, Frontiers Media SA.

2.2. Ditelluride bond-based GSH-responsive NPs

As a chalcogen, the chemical properties of tellurium are similar to sulfur. Compared with disulfide bonds, ditelluride bonds are more easily responsive to reducing substances, such as GSH, due to the lower bond energy. Although tellurium-containing polymers have been widely reported, nanoparticles based on ditellurium bonds are still in their infancy. In 2020, there was one case of ditellurium-based nanocarriers for sole chemotherapy. Sun and co-workers[88] prepared a ditelluride-containing PEGylated polycaprolactone modified with folic acid (FA) for active tumor targeting (Fig. 3). The polymer self-assembled to encapsulate DOX in aqueous solution, and the NPs exhibited GSH-responsive drug release due to the degradation of the ditelluride bonds. FA could promote the uptake of nanoparticles by 4T1 breast cancer cells, promoting the accumulation of the NPs at the tumor site and further enhancing the growth inhibitory effect on 4T1 tumors. Combination therapy based on ditelluride-containing polymers is expected to be carried out in the future.

2.3. Metal-ion-based GSH-responsive NPs

Besides, multivalent metal ions exhibit GSH responsiveness *via* redox reactions. The reduced metal ions can undergo a Fenton/Fenton-like reaction and react with H_2O_2 to generate more cytotoxic $^{\bullet}OH$ for chemodynamic therapy (CDT).[89–91] Common metal ions include Fe^{3+}/Fe^{2+}, Cu^{2+}/Cu^{+}, and Mn^{4+}/Mn^{2+}. Zhu

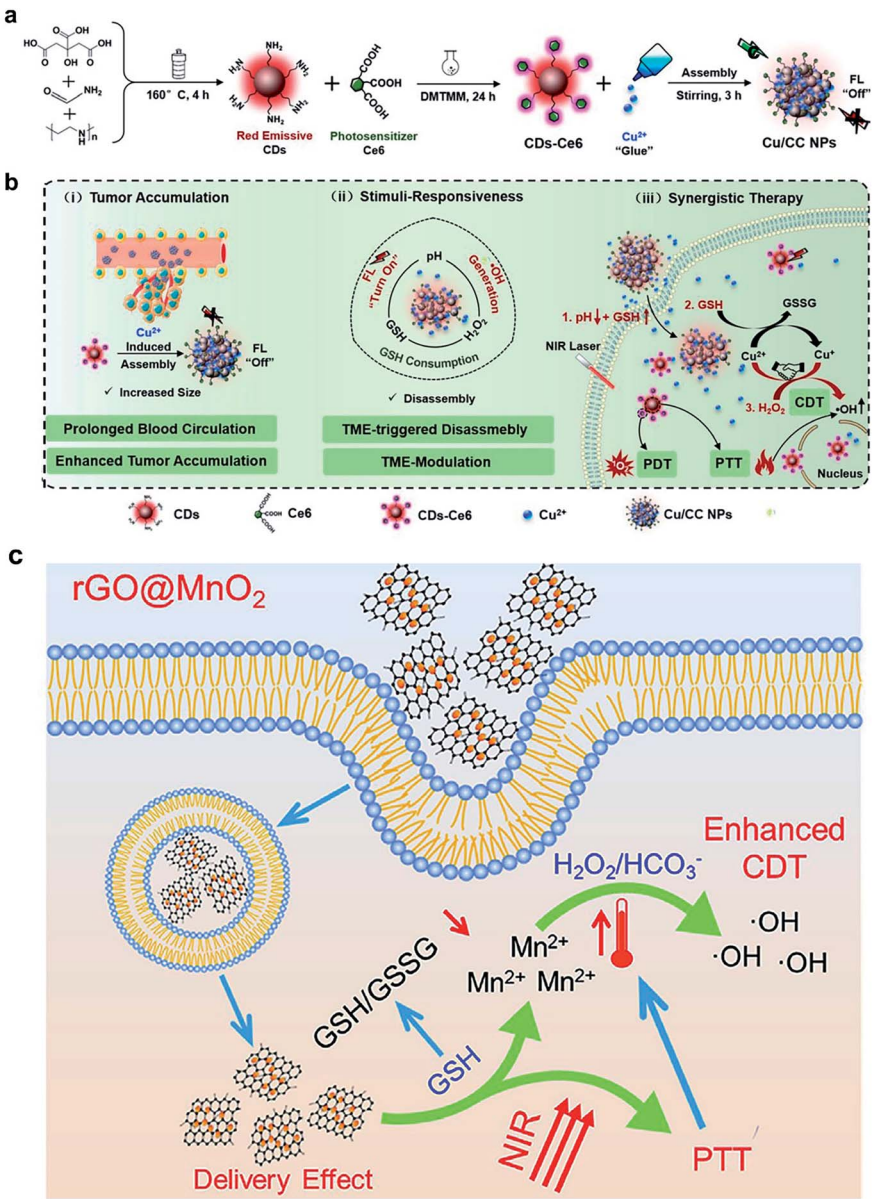

Fig. 5 Illustration of (a) the synthesis process of Cu/CC NPs and (b) their features for enhancing tumor accumulation, TME stimuli-response, and synergistic therapy.[93] (c) rGO@MnO_2-mediated PTT and photothermal/delivery effect enhanced CDT for synergistic cancer therapy.[94] Reproduced with permission from ref. 93 and 94. Copyright © 2020, Wiley-VCH. Copyright © 2021 Elsevier Ltd.

and co-workers[92] prepared an amphiphilic block copolymer *via* grafting polyethylene glycol (PEG) onto pH-responsive polyketal (PCK), which readily self-assembled into a vesicle to load the oil-soluble metal nanoclusters Au_1Ag_{24} as photosensitizers and water-soluble Fe^{3+}. In this work, the composite NPs with pH and GSH dual-responsive properties exhibited synergetic PTT and PDT under near-infrared light irradiation. Meanwhile, the Fe^{3+} ions acted as oxidants to consume GSH in order to prevent $^1O_2$ quenching. Besides, the formed Fe^{2+} ions underwent a Fenton reaction with endogenous H_2O_2 in tumors to generate $^{\cdot}OH$ for ferroptosis-based tumor therapy (Fig. 4). The multi-responsive, multimodal nanotherapeutic platform was confirmed as an effective cancer therapy both *in vitro* and *in vivo*.

Several other multivalent metal-ion pairs containing Cu^{2+}/Cu^{+} and Mn^{4+}/Mn^{2+} also display similar functions to Fe ions. Lin and co-workers[93] developed a responsive diagnosis and treatment integrated nanoplatform *via* the assembly of Ce6-modified carbon dots (CDs) with Cu^{2+} ions (Fig. 5a). The nanosystem showed quenched fluorescence and photosensitization due to the aggregation of Ce6, and the fluorescence imaging and photosensitization were restored once activated by pH/GSH. In addition, the introduction of Cu^{2+} provided additional CDT through reaction with H_2O_2, and also enhanced intracellular oxidative stress by consuming the tumor's intracellular GSH. The TME-responsive NPs offer a new strategy for imaging-guided multiple therapeutic modalities, including PDT, PTT and chemodynamic therapy (Fig. 5b). Bianco and co-workers[94] synthesized a GSH-responsive composite by anchoring negatively charged BSA-modified MnO_2 NPs on the surface of polyethyleneimine-modified reduced graphene oxide nanosheets (rGO NSs) *via* electrostatic interactions. The MnO_2 NPs were reduced to Mn^{2+} ions by intracellular GSH, which converted H_2O_2 to $^{\cdot}OH$ *via* a Fenton-like reaction for CDT and the rGO NSs further killed tumor cells due to PTT under NIR light irradiation (808 nm). Meanwhile, the high temperature induced by the photothermal conversion increased the rate of the Fenton-like reaction and enhanced the efficiency of CDT (Fig. 5c). Interestingly, the nanosystems exhibited a high lethality at low concentrations due to the presence of rGO, which facilitated the cellular uptake of MnO_2 NPs, thus further improving the biosafety.

3. ROS-responsive NPs for combined cancer therapy

A high level of ROS, especially H_2O_2, is a characteristic of TME.[95,96] The elevated H_2O_2 concentration in tumor tissue possess a strong oxidative capacity, making it a suitable stimulus for responsive NPs. The development of ROS-responsive nanoplatforms has attracted considerable attention.[64] Hence, we review several representative nanoplatforms based on thioketal-, arylboronic ester-, and aminoacrylate moieties.

3.1. Thioketal-based ROS-responsive NPs

Thioketal is a sulfur-based ROS-responsive moiety that has been shown to react with most ROS, including H_2O_2, $^1O_2$, $^{\cdot}OH$, and $O_2^{\cdot-}$.[97] Similar to disulfide bonds, thioketals are often grafted onto polymer chains to form polymer-based prodrugs or are used to link hydrophilic and hydrophobic prodrugs to generate amphiphilic small molecules. Sun and co-workers[98] synthesized an amphiphilic small molecule with the thioether- or thioketal-linked hypoxia-activated drugs PR104A and pyropheophorbide a (PPa). The amphiphilic small molecules self-assembled into nanoprodrugs that possessed a high dual drug-loading efficiency. Due to aggregation caused quenching (ACQ), 660 nm laser-excited PPa preferentially transferred electrons to the sulfur atoms of adjacent thioether or thioketal bonds *via* the photoinduced electron-transfer (PET) effect to form sulfur radical cations rather than generating $^1O_2$, which led to the cleavage of C–S bonds and the release of PR104A and PPa. With the dissociation of the nanoprodrug, the ACQ effect of PPa was relieved and ROS were generated under light to further accelerate the cleavage of the thioether or thioketal bonds, releasing PR104A and PPa. Additionally, aggravated hypoxia by PDT activated the efficacy of the prodrug PR104A for combination chemo-photodynamic therapy (Fig. 6a). Qian and co-workers[99] incorporated thioketal within the PEG chain to connect camptothecin (CPT) and grafted the photosensitizer PPa into the polymer to construct a ROS-responsive nanoprodrug system (Fig. 6b). The self-assembly of the conjugate prevented drug leakage during systemic circulation, and the PPa fluorescence signal precisely tracked NPs at the tumor sites. PPa generated ROS under near-infrared laser irradiation, which cleaved thioketal to release CPT in a controllable and on-demand manner. The combined CPT-mediated chemotherapy and PPA-induced PDT suppressed the tumor growth.

3.2. Arylboronic ester-based ROS-responsive NPs

Arylboronic ester is also a common ROS-responsive group used in the design of stimuli-responsive nanomaterials. H_2O_2 nucleophilically attacks the boron center, which is further hydrolyzed to release phenol and boric acid.[100,101] The nanoplatform-installed arylboronic ester moieties were degraded to release the cargo in the presence of H_2O_2. Cui and co-workers[102] reported a light and ROS dual-responsive multistage nanocarrier consisting of phenylboronic acid-crosslinked polyethylene glycol-polycaprolactone, indocyanine green (ICG), and pyridine endoperoxide (PE) (Fig. 7a). Here, ICG acted as both a photosensitizer and a photothermal agent to generate ROS and heat. The excessive ROS in the tumor broke the phenylboronic acid to accelerate the release of ICG and PE, and the elevated temperature induced PE to continuously release oxygen for relieving deep tumor hypoxia to promote PDT. The nanocarriers generated multistage responses *in situ* to induce tumor double apoptosis, maximizing the therapeutic effect of PTT/PDT.

Arylboronic ester is a component of a proalkylating agent that can be activated by H_2O_2 and can irreversibly deplete GSH to increase oxidative stress in tumor cells.[103,104] Yan and co-workers[105] synthesized silica-coated bismuth NPs with premixed H_2O_2-responsive arylboronic ester-containing prodrugs and lauric acid on the surfaces. Lauric acid was melted under near-infrared light irradiation to release the prodrug, which was

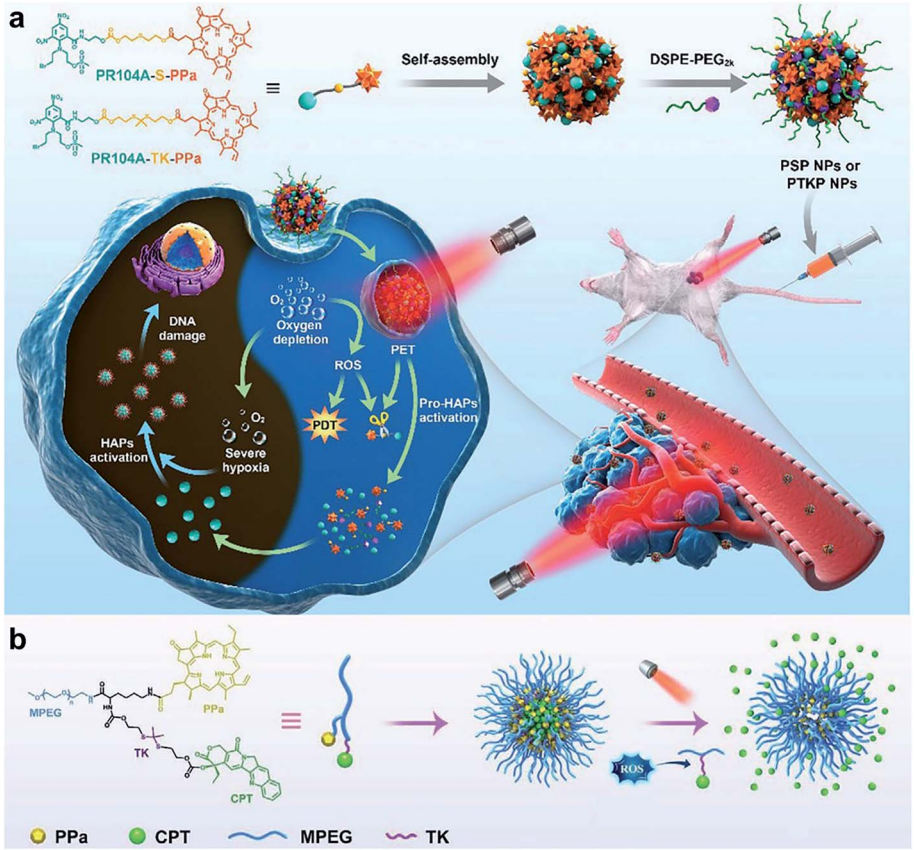

Fig. 6 (a) Schematic illustration of the preparation of self-assembled heterodimeric prodrug-NPs, the light-triggered dual-modality activation of the prodrug-NPs, and the PDT-induced activation of HAPs.[98] (b) Schematic illustration of the MPEG-(TK-CPT)-PPa NPs for photo-triggered ROS-activatable CPT prodrug release and local tumor therapy.[99] Reproduced with permission from ref. 98 and 99. Copyright © 2020, The Royal Society of Chemistry. Copyright © 2020, Wiley-VCH.

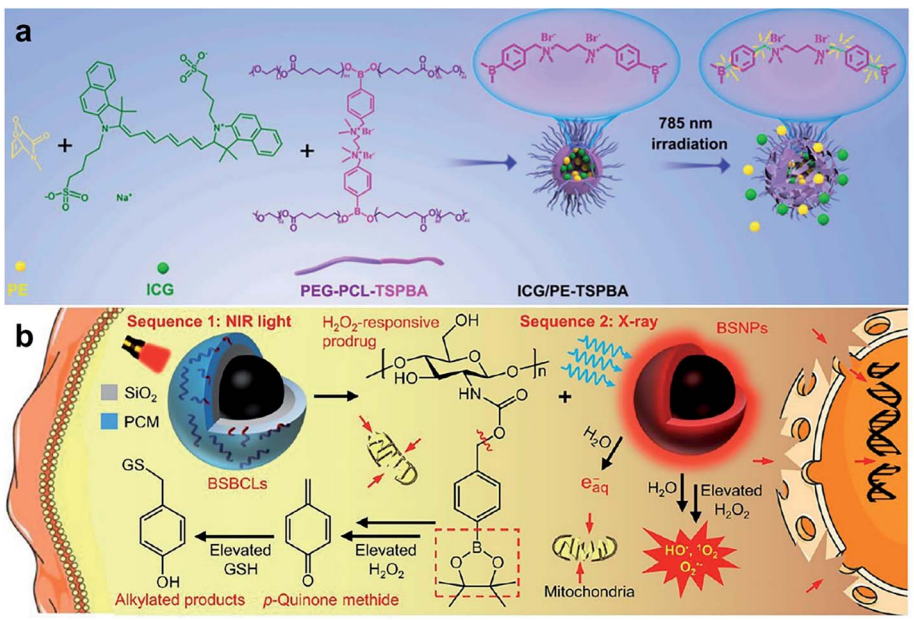

Fig. 7 (a) Fabrication and responsive breakage of the nanocarrier ICG/PE-TSPBA.[102] (b) Schematic illustration of the BBSLs NPs for NIR- and X-ray-triggered ROS-activatable prodrug release.[105] Reproduced with permission from ref. 102 and 105. Copyright © 2021, Elsevier Ltd. Copyright © 2021, American Chemical Society.

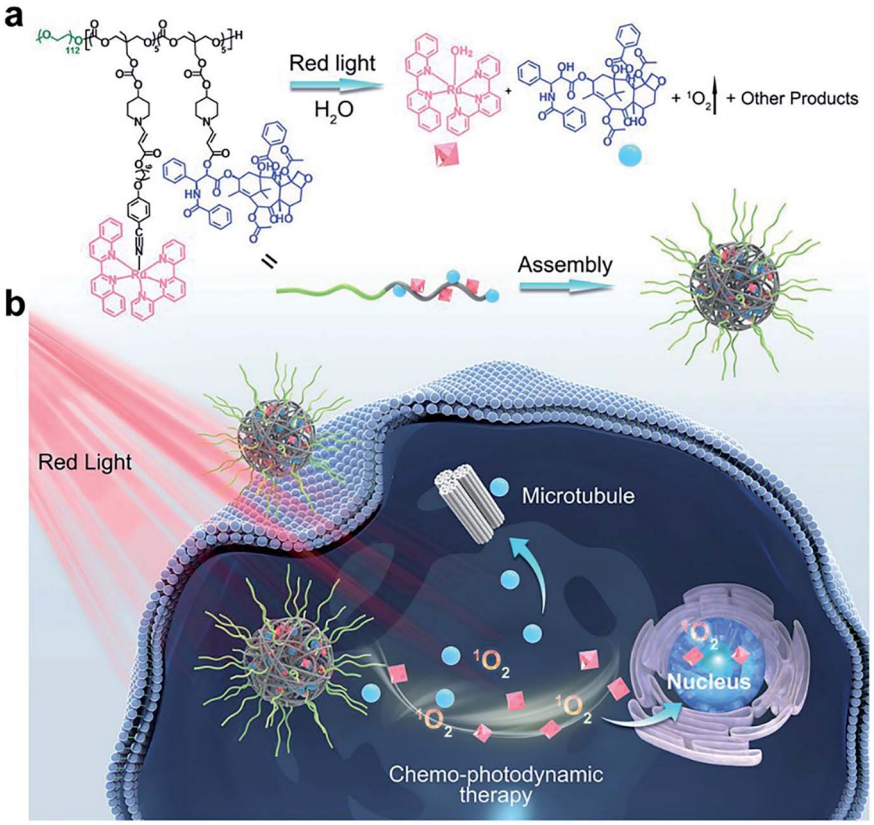

Fig. 8 (a) Chemical structure of the amphiphilic copolymer poly (Ru/PTX). Red-light irradiation induced cleavage of the Ru complex, the generation of $^1O_2$, and release of the anticancer drug PTX. (b) Schematic illustration of the self-assembly, cell internalization, and chemo-photodynamic therapy using poly (Ru/PTX).[108] Reproduced with permission from ref. 108, copyright © 2021, Wiley-VCH.

converted into the electrophilic *p*-quinone methyl ether in the presence of H_2O_2, irreversibly depleting GSH and enhancing tumor oxidative stress. The generated heat promoted blood flow into the tumor tissue and relieved the hypoxic microenvironment. Bismuth NPs, as radiosensitizers, generated a large amount of ROS under X-ray irradiation, synergistically inducing

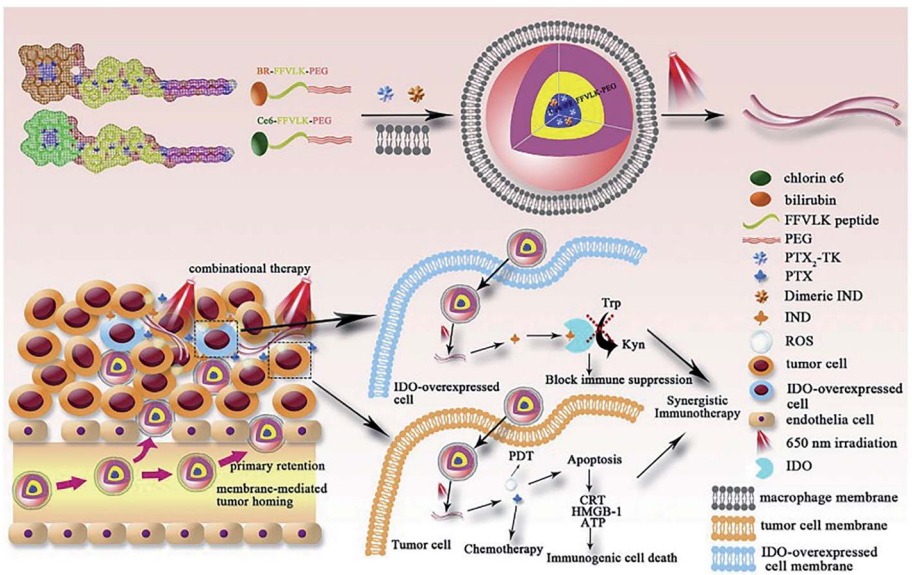

Fig. 9 Illustration of the construction of I–P@NPs@M and its function in the tumor region.[111] Reproduced with permission from ref. 111, copyright © 2020, Elsevier. Ltd.

cell death through DNA fragmentation and mitochondria-mediated apoptosis (Fig. 7b). This strategy effectively inhibited tumor growth *in vivo* with high tumor specificity and reduced side effects.

3.3. Aminoacrylate-based ROS-responsive NPs

Aminoacrylate is another ROS-responsive group, which is sensitive to $^1O_2$. The β-aminoacrylate linkage undergoes fast oxidative degradation, resulting in the cleavage of ester bonds.[106,107] Following the mechanism, our group[108] synthesized a red-light-responsive metallopolymer with a biodegradable backbone structure containing a Ru complex as the photosensitizer and a chemo-drug paclitaxel (PTX) linked *via* $^1O_2$ activatable aminoacrylate linker (Fig. 8a). Under the irradiation of 650 nm red light, the cyano coordination bond between the polymer and the Ru ligand was cut, which then released the Ru complex to generate $^1O_2$ for PDT. Subsequently, the generated $^1O_2$ triggered cleavage of the β-aminoacrylate linker, resulting in the release of PTX for chemotherapy (Fig. 8b). The sequential dual-drug-release strategy minimized the premature drug release *in vivo* and enabled combined chemotherapy and PDT for enhanced anticancer efficiency.

3.4. Bilirubin-based ROS-responsive NPs

Bilirubin (BR) is an endogenous small molecule that can be converted from hydrophilic to hydrophobic with ROS. In some reports, BR as a ROS-responsive group was used to design nanocarriers for controlled anticancer agent delivery.[109,110] Gao and co-workers[111] used BR or Ce6 as the hydrophobic end, PEG as the hydrophilic tail, and the polypeptide chain for hydrogen bond formation to synthesize two amphiphilic triblock molecules, which co-assembled into micelles to encapsulate the prodrug PTX and pro-immune reagent indoximod (IND). The NPs were further coated on the macrophage membrane to facilitate tumor targeting. ROS were generated by Ce6 upon 650 nm laser irradiation, triggering the transformation of the micelles into nanofibers and facilitating the release of anticancer agents. Chemo-photodynamic therapy significantly inhibited tumor proliferation and triggered immunogenic cell death (ICD) effects, which were combined with IND to activate the immune response (Fig. 9).

4. ROS and GSH dual-responsive NPs for combined cancer therapy

Due to the heterogeneity of tumors, different concentrations of ROS and GSH are found in various tumors, and even different GSH/ROS levels are found in different regions of the same tumor.[112] Thus, GSH or ROS single-responsive DDSs may be limited in selectivity and response efficiency.[113,114] Compared with single-responsive NPs, redox dual-triggered NPs exhibit a faster response rate and higher drug-release efficiency. Therefore, DDSs with dual responsiveness are more promising in diverse pathological conditions.[115,116] Some chemical moieties can react with ROS and GSH simultaneously, such as diselenide and α-dicarbonyl thioether, which are utilized for the design of responsive NPs.

4.1. Diselenide-based ROS and GSH dual-responsive NPs

As known, diselenide linkers can not only be cleaved and oxidized to seleninic acid by ROS, but also reduced to selenol in the presence of a reducing agent.[117,118] So far, diselenide bonds have been widely used in inorganic and polymeric nanomaterial frameworks for the controlled release of cargoes. Shao and co-workers[119] designed diselenide-bond-bridged mesoporous silica nanoparticles (MSNs) that possessed redox dual-responsive properties for cancer therapeutics (Fig. 10a). The cytotoxic RNase A was encapsulated into the pores of diselenide bond-bridged MSNs and released *via* matrix degradation in the presence of ROS or GSH. The NPs were endowed with homologous targeting features after being coated on the cancer cell membrane. The diselenide bond-bridged MSNs exhibited high anticancer properties *in vitro* and *in vivo*. The research group[120] found that diselenide bond-bridged MSNs also possessed X-ray responsiveness. The MSNs showed material degradation to control the release of DOX with low-dose X-ray irradiation, which resulted in an ICD effect for chemo-immunotherapy to inhibit tumor growth and metastasis (Fig. 10b). Further, our group[121] utilized the diselenide bond-bridged MSNs to co-encapsulate the chemo-drug DOX and photosensitizer methylene blue (MB) for red-light-responsive cascade-amplifying chemo-photodynamic-immunotherapy. Under 660 nm red-light irradiation, MB generated ROS, which resulted in a collapse of the organosilica matrix and release of the dual drug for combined chemotherapy and PDT. Interestingly, the cascaded chemo-photodynamic therapy enhanced ICD and the antitumor immune responses, which suppressed tumor growth, metastasis, and recurrence combined with anti-PD-1 (Fig. 10c).

5. Conclusion and perspective

Redox-responsive NPs have exhibited great potential in DDSs and targeted tumor combined therapy due to their easy preparation, specificity, easy modifiability, and low toxicity. In the past three years, researchers have made great efforts to develop GSH-responsive NPs based on disulfide bonds, ditelluride bonds, and metal ions, ROS-responsive NPs based on thioketal, arylboronic ester, aminoacrylate, and BR, as well as ROS/GSH dual-responsive NPs containing diselenide and dicarbonyl thioether groups. These reviewed examples demonstrated excellent anticancer effects both *in vitro* and *in vivo*. Causing oxidative stress can result in tumor cell apoptosis through disruption of the redox balance in cancer cells; thus, the modulation of ROS production combined with ROS-activated nanomedicine could trigger cascades of the therapeutic effects on tumor tissues. Therefore, many ROS-responsive nanocarriers have been developed and made significant progress in cancer therapy. In addition, given that GSH plays a role in the quenching of ROS, a strategy to amplify oxidative stress by promoting the generation of ROS and the consumption of GSH was proposed to inhibit tumor growth. These designs have attracted great interest in controlled drug release to enhance therapeutic efficacy.

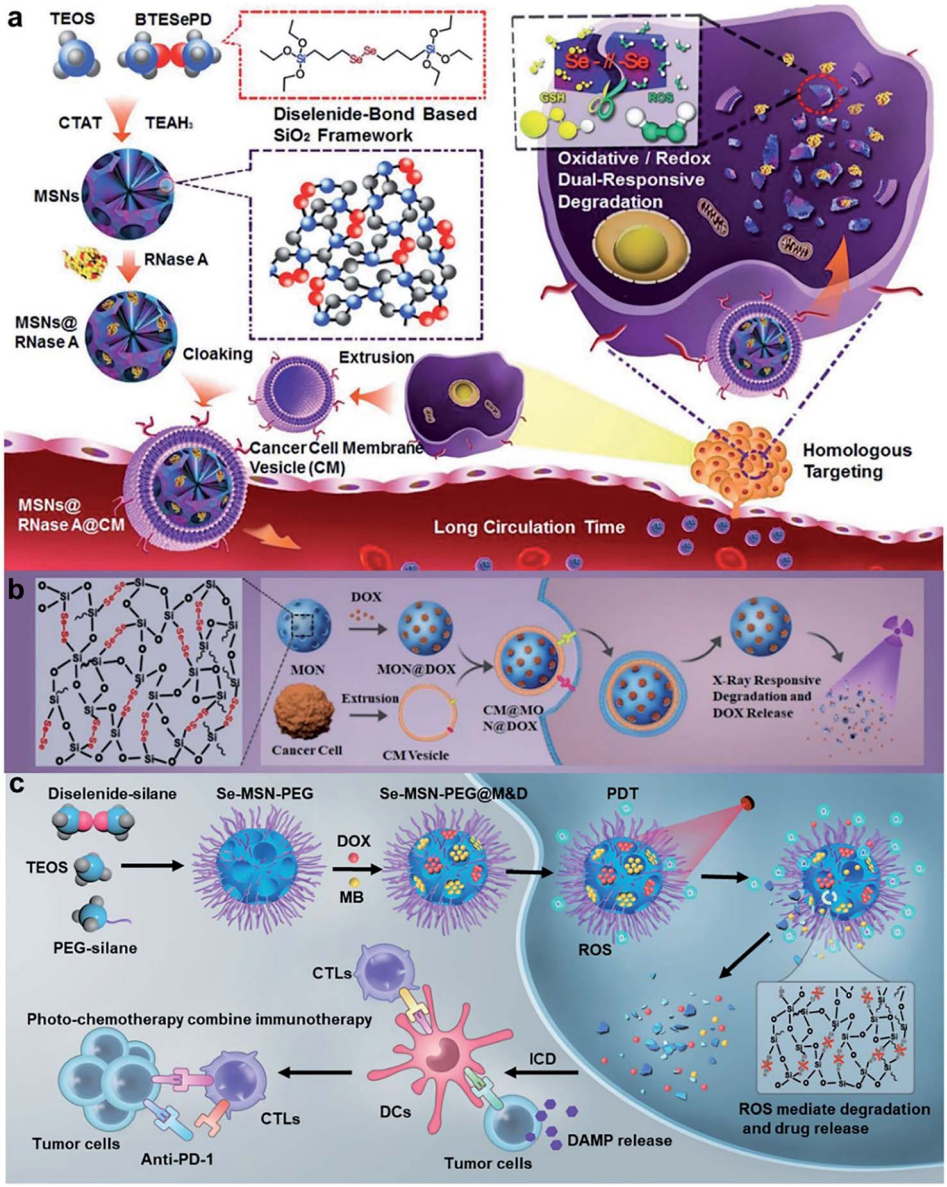

Fig. 10 (a) Schematic illustration of the synthesis procedure of biodegradable diselenide-bridged MSNs and their application for dual-responsive, cancer cell-membrane-mimetic protein delivery.[119] (b) Schematic of the synthesis of diselenide-bond-bridged MONs for low-dose X-ray radiation-controllable drug release.[120] (c) Schematic of the synthetic procedure of Se-MSN-PEG with cascading drug release and amplifying ICD manners and their application for efficient and safe cancer chemo-photo-immunotherapy.[121] Reproduced with permission from ref. 119, 120 and 121. Copyright © 2018, 2020, Wiley-VCH. Copyright © 2022, Elsevier Ltd.

Despite the rapid development of redox-responsive nanoplatforms, the research is still in the preclinical stage with many obstacles for clinical use. First, although redox-responsive NPs have exhibited better antitumor ability than common DDSs due to their specificity to redox conditions, their targeting ability mainly depends on the EPR effect, which requires further improvement. Studies have shown that combining tumor-specific ligands or cancer-cell-derived membrane with DDSs can largely enhance the tumor-targeting ability.[122,123,124,125,126] Thus, redox-responsive NPs with enhanced tumor-targeting ability are expected to be investigated and developed in the near future. Second, the biosafety of NPs is a matter of great concern. The biocompatibility of most existing NPs was only investigated during the treatment. The fate of the NPs *in vivo* after the therapeutic agents are released needs to be studied, including their metabolic pathways and long-term side effects. Only redox-responsive NPs with excellent biosafety can be confidently used in future clinical research. Third, the tumor models used in the current research were constructed in mice, but the microenvironment of human tumors is different. In order to achieve clinical therapeutic use, it is necessary to better understand the human tumor microenvironment and to design related redox-responsive NPs. With the enhancement of tumor specificity, biosafety, and sensitivity, redox-responsive NPs will be promising for more desirable therapeutic modalities, enabling their future clinical applications.

Conflicts of interest

There are no conflicts to declare.

References

1 R. L. Siegel, K. D. Miller and A. Jemal, *Ca-Cancer J. Clin.*, 2020, **70**, 7–30.
2 P. Agostinis, K. Berg, K. A. Cengel, T. H. Foster, A. W. Girotti, S. O. Gollnick, S. M. Hahn, M. R. Hamblin, A. Juzeniene, D. Kessel, M. Korbelik, J. Moan, P. Mroz, D. Nowis, J. Piette, B. C. Wilson and J. Golab, *Ca-Cancer J. Clin.*, 2011, **61**, 250–281.
3 H. Shi and P. J. Sadler, *Br. J. Cancer*, 2020, **123**, 871–873.
4 Q. Zheng, X. Liu, Y. Zheng, K. W. K. Yeung, Z. Cui, Y. Liang, Z. Li, S. Zhu, X. Wang and S. Wu, *Chem. Soc. Rev.*, 2021, **50**, 5086–5125.
5 G. Lan, K. Ni and W. Lin, *Coord. Chem. Rev.*, 2019, **379**, 65–81.
6 V. T. DeVita Jr and E. Chu, *Cancer Res.*, 2008, **68**, 8643–8653.
7 S. B. Park, D. Goldstein, A. V. Krishnan, C. S. Lin, M. L. Friedlander, J. Cassidy, M. Koltzenburg and M. C. Kiernan, *Ca-Cancer J. Clin.*, 2013, **63**, 419–437.
8 G. S. Karagiannis, J. S. Condeelis and M. H. Oktay, *Clin. Exp. Metastasis*, 2018, **35**, 269–284.
9 M. Yu, D. Su, Y. Yang, L. Qin, C. Hu, R. Liu, Y. Zhou, C. Yang, X. Yang, G. Wang and H. Gao, *ACS Appl. Mater. Interfaces*, 2019, **11**, 176–186.
10 K. Nurgali, R. T. Jagoe and R. Abalo, *Front. Pharmacol.*, 2018, **9**, 245.
11 X. Li, J. F. Lovell, J. Yoon and X. Chen, *Nat. Rev. Clin. Oncol.*, 2020, **17**, 657–674.
12 D. Xi, M. Xiao, J. Cao, L. Zhao, N. Xu, S. Long, J. Fan, K. Shao, W. Sun, X. Yan and X. Peng, *Adv. Mater.*, 2020, **32**, 1907855.
13 D. Xi, N. Xu, X. Xia, C. Shi, X. Li, D. Wang, S. Long, J. Fan, W. Sun and X. Peng, *Adv. Mater.*, 2022, **34**, 2106797.
14 Y. Qin, F. Tong, W. Zhang, Y. Zhou, S. He, R. Xie, T. Lei, Y. Wang, S. Peng, Z. Li, J. Leong, H. Gao and L. Lu, *Adv. Funct. Mater.*, 2021, **31**, 2104645.
15 X.-Q. Zhou, M. Xiao, V. Ramu, J. Hilgendorf, X. Li, P. Papadopoulou, M. A. Siegler, A. Kros, W. Sun and S. Bonnet, *J. Am. Chem. Soc.*, 2020, **142**, 10383–10399.
16 S.-Y. Qin, Y.-J. Cheng, Q. Lei, A.-Q. Zhang and X.-Z. Zhang, *Biomaterials*, 2018, **171**, 178–197.
17 W. Sang, Z. Zhang, Y. Dai and X. Chen, *Chem. Soc. Rev.*, 2019, **48**, 3771–3810.
18 Y. Wang, J. Liu, X. Ma and X.-J. Liang, *Nano Res.*, 2018, **11**, 2932–2950.
19 H. Lei, X. Wang, S. Bai, F. Gong, N. Yang, Y. Gong, L. Hou, M. Cao, Z. Liu and L. Cheng, *ACS Appl. Mater. Interfaces*, 2020, **12**, 52370–52382.
20 J. Liu, M. Wu, Y. Pan, Y. Duan, Z. Dong, Y. Chao, Z. Liu and B. Liu, *Adv. Funct. Mater.*, 2020, **30**, 1908865.
21 J. Park, Y. Choi, H. Chang, W. Um, J. H. Ryu and I. C. Kwon, *Theranostics*, 2019, **9**, 8073–8090.
22 S. S. Lucky, K. C. Soo and Y. Zhang, *Chem. Rev.*, 2015, **115**, 1990–2042.
23 A. S. Thakor and S. S. Gambhir, *Ca-Cancer J. Clin.*, 2013, **63**, 395–418.
24 S. Guo, K. Li, B. Hu, C. Li, M. Zhang, A. Hussain, X. Wang, Q. Cheng, F. Yang, K. Ge, J. Zhang, J. Chang, X. J. Liang, Y. Weng and Y. Huang, *Exploration*, 2021, **1**, 35–49.
25 K. Y. W. Teo, C. Sevencan, Y. A. Cheow, S. Zhang, D. T. Leong and W. S. Toh, *Small Science*, 2022, **2**, 2100116.
26 B. Zhang, D. Zheng, S. Yiming, K. Oyama, M. Ito, M. Ikari, T. Kigawa, T. Mikawa and T. Miyake, *Small Science*, 2021, **1**, 2100069.
27 Y. Wang, Y. Zhang, J. Wang and X. J. Liang, *Adv. Drug Delivery Rev.*, 2019, **143**, 161–176.
28 Y. Yamada, Satrialdi, M. Hibino, D. Sasaki, J. Abe and H. Harashima, *Adv. Drug Delivery Rev.*, 2020, **154–155**, 187–209.
29 L. Duan, L. Yang, J. Jin, F. Yang, D. Liu, K. Hu, Q. Wang, Y. Yue and N. Gu, *Theranostics*, 2020, **10**, 462–483.
30 W. Cai, J. Wang, C. Chu, W. Chen, C. Wu and G. Liu, *Adv. Sci.*, 2019, **6**, 1801526.
31 Z. R. Lu, V. E. A. Laney, R. Hall and N. Ayat, *Adv. Healthcare Mater.*, 2021, **10**, 2001294.
32 C. Y. Ang, S. Y. Tan, C. Teh, J. M. Lee, M. F. Wong, Q. Qu, L. Q. Poh, M. Li, Y. Zhang, V. Korzh and Y. Zhao, *Small*, 2017, **13**, 1602379.
33 J. Li, X. Huang, X. Zhao, L. J. Chen and X. P. Yan, *Angew. Chem., Int. Ed.*, 2021, **60**, 2398–2405.
34 M. He, F. Chen, D. Shao, P. Weis, Z. Wei and W. Sun, *Biomaterials*, 2021, **275**, 120915.
35 F. Chen, F. Zhang, D. Shao, W. Zhang, L. Zheng, W. Wang, W. Yang, Z. Wang, J. Chen, W.-f. Dong, F. Xiao and Y. Wu, *Appl. Mater. Today*, 2020, **19**, 100558.
36 N. M. Anderson and M. C. Simon, *Curr. Biol.*, 2020, **30**, R921–R925.
37 S. Yang and H. Gao, *Pharmacol. Res.*, 2017, **126**, 97–108.
38 Y. Zhou, X. Chen, J. Cao and H. Gao, *J. Mater. Chem. B*, 2020, **8**, 6765–6781.
39 C. Gong, X. Zhang, M. Shi, F. Li, S. Wang, Y. Wang, Y. Wang, W. Wei and G. Ma, *Adv. Sci.*, 2021, **8**, 2002787.
40 E. Perez-Herrero and A. Fernandez-Medarde, *Acta Pharm. Sin. B*, 2021, **11**, 2243–2264.
41 S. Chen, D. Li, X. Du, X. He, M. Huang, Y. Wang, X. Yang and J. Wang, *Nano Today*, 2020, **35**, 100924.
42 J. Zhao, Y. Y. Peng, D. Diaz-Dussan, J. White, W. Duan, L. Kong, R. Narain and X. Hao, *Mol. Pharm.*, 2022, **19**, 1766–1777.
43 J. Mu, H. Zhong, H. Zou, T. Liu, N. Yu, X. Zhang, Z. Xu, Z. Chen and S. Guo, *J. Controlled Release*, 2020, **326**, 265–275.
44 W. R. Wilson and M. P. Hay, *Nat. Rev. Cancer*, 2011, **11**, 393–410.
45 A. Patel and S. Sant, *Biotechnol. Adv.*, 2016, **34**, 803–812.
46 D. Cui, J. Huang, X. Zhen, J. Li, Y. Jiang and K. Pu, *Angew. Chem., Int. Ed.*, 2019, **58**, 5920–5924.
47 S. Zhou, X. Hu, R. Xia, S. Liu, Q. Pei, G. Chen, Z. Xie and X. Jing, *Angew. Chem., Int. Ed.*, 2020, **59**, 23198–23205.

48 Q. Mou, Y. Ma, F. Ding, X. Gao, D. Yan, X. Zhu and C. Zhang, *J. Am. Chem. Soc.*, 2019, **141**, 6955–6966.
49 L. Luo, Z. Yin, Y. Qi, S. Liu, Y. Yi, X. Tian, Y. Wu, D. Zhong, Z. Gu, H. Zhang and K. Luo, *Appl. Mater. Today*, 2021, **23**, 100996.
50 Y. Liu, Y. Lu, X. Zhu, C. Li, M. Yan, J. Pan and G. Ma, *Biomaterials*, 2020, **242**, 119933.
51 J. Choi, M. K. Shim, S. Yang, H. S. Hwang, H. Cho, J. Kim, W. S. Yun, Y. Moon, J. Kim, H. Y. Yoon and K. Kim, *ACS Nano*, 2021, **15**, 12086–12098.
52 D. Li, R. Zhang, G. Liu, Y. Kang and J. Wu, *Adv. Healthcare Mater.*, 2020, **9**, 2000605.
53 P. H. Hsu and A. Almutairi, *J. Mater. Chem. B*, 2021, **9**, 2179–2188.
54 R. Li, F. Peng, J. Cai, D. Yang and P. Zhang, *Asian J. Pharm. Sci.*, 2020, **15**, 311–325.
55 T. Lei, Z. Yang, X. Xia, Y. Chen, X. Yang, R. Xie, F. Tong, X. Wang and H. Gao, *Acta Pharm. Sin. B*, 2021, **11**, 4032–4044.
56 S. H. Lee, M. K. Gupta, J. B. Bang, H. Bae and H. J. Sung, *Adv. Healthcare Mater.*, 2013, **2**, 908–915.
57 C. R. Reczek and N. S. Chandel, *Annu. Rev. Cancer Biol.*, 2017, **1**, 79–98.
58 J. Wang, L. Liu, L. Yin and L. Chen, *J. Biomed. Mater. Res., Part A*, 2018, **106**, 2955–2962.
59 G. Liu, Z. Bao and J. Wu, *Chin. Chem. Lett.*, 2020, **31**, 1817–1821.
60 J. M. Estrela, A. Ortega and E. Obrador, *Crit. Rev. Clin. Lab. Sci.*, 2006, **43**, 143–181.
61 J. A. Cook, D. Gius, D. A. Wink, M. C. Krishna, A. Russo and J. B. Mitchell, *Semin. Radiat. Oncol.*, 2004, **14**, 259–266.
62 X. Zhong, X. Wang, L. Cheng, Y. Tang, G. Zhan, F. Gong, R. Zhang, J. Hu, Z. Liu and X. Yang, *Adv. Funct. Mater.*, 2020, **30**, 1907954.
63 C. R. Corso and A. Acco, *Crit. Rev. Oncol. Hematol.*, 2018, **128**, 43–57.
64 G. Saravanakumar, J. Kim and W. J. Kim, *Adv. Sci.*, 2017, **4**, 1600124.
65 M. S. Shim and Y. Xia, *Angew. Chem., Int. Ed.*, 2013, **52**, 6926–6929.
66 M. Bio, G. Nkepang and Y. You, *Chem. Commun.*, 2012, **48**, 6517–6519.
67 C. Lin, F. Tong, R. Liu, R. Xie, T. Lei, Y. Chen, Z. Yang, H. Gao and X. Yu, *Acta Pharm. Sin. B*, 2020, **10**, 2348–2361.
68 M. H. Lee, Z. Yang, C. W. Lim, Y. H. Lee, S. Dongbang, C. Kang and J. S. Kim, *Chem. Rev.*, 2013, **113**, 5071–5109.
69 J. Li, L. Jiao, W. Xu, H. Yan, G. Chen, Y. Wu, L. Hu and W. Gu, *Sens. Actuators, B*, 2021, **329**, 129247.
70 H. Pelicano, D. Carney and P. Huang, *Drug Resist. Updates*, 2004, **7**, 97–110.
71 F. Liu, T. Bing, D. Shangguan, M. Zhao and N. Shao, *Anal. Chem.*, 2016, **88**, 10631–10638.
72 C. Shi, M. Li, Z. Zhang, Q. Yao, K. Shao, F. Xu, N. Xu, H. Li, J. Fan, W. Sun, J. Du, S. Long, J. Wang and X. Peng, *Biomaterials*, 2020, **233**, 119755.
73 Z. Deng, Y. Qian, Y. Yu, G. Liu, J. Hu, G. Zhang and S. Liu, *J. Am. Chem. Soc.*, 2016, **138**, 10452–10466.
74 Y. H. Kim, X. T. Cao, S.-S. Hong, Y. S. Gal and K. T. Lim, *Mol. Cryst. Liq. Cryst.*, 2016, **635**, 107–113.
75 M. Wen, J. Ouyang, C. Wei, H. Li, W. Chen and Y. N. Liu, *Angew. Chem., Int. Ed.*, 2019, **58**, 17425–17432.
76 X. Guo, Y. Cheng, X. Zhao, Y. Luo, J. Chen and W. E. Yuan, *J. Nanobiotechnol.*, 2018, **16**, 74.
77 F. Gong, M. Chen, N. Yang, Z. Dong, L. Tian, Y. Hao, M. Zhuo, Z. Liu, Q. Chen and L. Cheng, *Adv. Funct. Mater.*, 2020, **30**, 2002753.
78 L. S. Lin, J. Song, L. Song, K. Ke, Y. Liu, Z. Zhou, Z. Shen, J. Li, Z. Yang, W. Tang, G. Niu, H. H. Yang and X. Chen, *Angew. Chem., Int. Ed.*, 2018, **57**, 4902–4906.
79 L. H. Fu, Y. Wan, C. Qi, J. He, C. Li, C. Yang, H. Xu, J. Lin and P. Huang, *Adv. Mater.*, 2021, **33**, 2006892.
80 L. Lu, X. Zhao, T. Fu, K. Li, Y. He, Z. Luo, L. Dai, R. Zeng and K. Cai, *Biomaterials*, 2020, **230**, 119666.
81 S. Li, P. E. Saw, C. Lin, Y. Nie, W. Tao, O. C. Farokhzad, L. Zhang and X. Xu, *Biomaterials*, 2020, **234**, 119760.
82 X. Yi, J. J. Hu, J. Dai, X. Lou, Z. Zhao, F. Xia and B. Z. Tang, *ACS Nano*, 2021, **15**, 3026–3037.
83 K. Luo, W. Guo, Y. Yu, S. Xu, M. Zhou, K. Xiang, K. Niu, X. Zhu, G. Zhu, Z. An, Q. Yu and Z. Gan, *J. Controlled Release*, 2020, **326**, 25–37.
84 L. Luo, Y. Qi, H. Zhong, S. Jiang, H. Zhang, H. Cai, Y. Wu, Z. Gu, Q. Gong and K. Luo, *Acta Pharm. Sin. B*, 2022, **12**, 424–436.
85 X. Xie, C. Zhan, J. Wang, F. Zeng and S. Wu, *Small*, 2020, **16**, 2003451.
86 Y. Yang, B. Sun, S. Zuo, X. Li, S. Zhou, L. Li, C. Luo, H. Liu, M. Cheng, Y. Wang, S. Wang, Z. He and J. Sun, *Sci. Adv.*, 2020, **6**, eabc1725.
87 W. Feng, Y. Lv, Z. Chen, F. Wang, Y. Wang, Y. Pei, W. Jin, C. Shi, Y. Wang, Y. Qu, W. Ji, L. Pu, X.-W. Liu and Z. Pei, *Chem. Eng. J.*, 2021, **417**, 129178.
88 Z. Pang, J. Zhou and C. Sun, *Front. Chem.*, 2020, **8**, 156.
89 H. Deng, Z. Yang, X. Pang, C. Zhao, J. Tian, Z. Wang and X. Chen, *Nano Today*, 2022, **42**, 101337.
90 X. Lin, R. Zhu, Z. Hong, X. Zhang, S. Chen, J. Song and H. Yang, *Adv. Funct. Mater.*, 2021, **31**, 2101278.
91 Y. Yan, Y. Hou, H. Zhang, W. Gao, R. Han, J. Yu, L. Xu and K. Tang, *Colloids Surf., B*, 2021, **208**, 112103.
92 H. Cheng, X. Wang, X. Liu, X. Wang, H. Wen, Y. Cheng, A. Xie, Y. Shen, R. Tang and M. Zhu, *Nanoscale*, 2021, **13**, 10816–10828.
93 S. Sun, Q. Chen, Z. Tang, C. Liu, Z. Li, A. Wu and H. Lin, *Angew. Chem., Int. Ed.*, 2020, **59**, 21041–21048.
94 B. Ma, Y. Nishina and A. Bianco, *Carbon*, 2021, **178**, 783–791.
95 V. J. Thannickal and B. L. Fanburg, *Am. J. Physiol.: Lung Cell. Mol. Physiol.*, 2000, **279**, L1005–L1028.
96 S. Parvez, M. J. C. Long, J. R. Poganik and Y. Aye, *Chem. Rev.*, 2018, **118**, 8798–8888.
97 X. Xu, P. E. Saw, W. Tao, Y. Li, X. Ji, S. Bhasin, Y. Liu, D. Ayyash, J. Rasmussen, M. Huo, J. Shi and O. C. Farokhzad, *Adv. Mater.*, 2017, **29**, 1700141.

98 D. Zhao, W. Tao, S. Li, L. Li, Y. Sun, G. Li, G. Wang, Y. Wang, B. Lin, C. Luo, Y. Wang, M. Cheng, Z. He and J. Sun, *Nanoscale Horiz.*, 2020, **5**, 886–894.
99 B. Chu, Y. Qu, X. He, Y. Hao, C. Yang, Y. Yang, D. Hu, F. Wang and Z. Qian, *Adv. Funct. Mater.*, 2020, **30**, 2005918.
100 C.-C. Song, R. Ji, F.-S. Du and Z.-C. Li, *Macromolecules*, 2013, **46**, 8416–8425.
101 M. Zhang, C. C. Song, S. Su, F. S. Du and Z. C. Li, *ACS Appl. Mater. Interfaces*, 2018, **10**, 7798–7810.
102 H. Luo, C. Huang, J. Chen, H. Yu, Z. Cai, H. Xu, C. Li, L. Deng, G. Chen and W. Cui, *Biomaterials*, 2021, **279**, 121194.
103 C. Lux, S. Joshi-Barr, T. Nguyen, E. Mahmoud, E. Schopf, N. Fomina and A. Almutairi, *J. Am. Chem. Soc.*, 2012, **134**, 15758–15764.
104 A. Gennari, C. Gujral, E. Hohn, E. Lallana, F. Cellesi and N. Tirelli, *Bioconjugate Chem.*, 2017, **28**, 1391–1402.
105 H. Xiang, Y. Wu, X. Zhu, M. She, Q. An, R. Zhou, P. Xu, F. Zhao, L. Yan and Y. Zhao, *J. Am. Chem. Soc.*, 2021, **143**, 11449–11461.
106 M. Bio, P. Rajaputra, G. Nkepang, S. G. Awuah, A. M. Hossion and Y. You, *J. Med. Chem.*, 2013, **56**, 3936–3942.
107 P. Thapa, M. Li, M. Bio, P. Rajaputra, G. Nkepang, Y. Sun, S. Woo and Y. You, *J. Med. Chem.*, 2016, **59**, 3204–3214.
108 M. He, G. He, P. Wang, S. Jiang, Z. Jiao, D. Xi, P. Miao, X. Leng, Z. Wei, Y. Li, Y. Yang, R. Wang, J. Du, J. Fan, W. Sun and X. Peng, *Adv. Sci.*, 2021, **8**, 2103334.
109 X. Yang, C. Hu, F. Tong, R. Liu, Y. Zhou, L. Qin, L. Ouyang and H. Gao, *Adv. Funct. Mater.*, 2019, **29**, 1901896.
110 R. Liu, M. Yu, X. Yang, C. S. Umeshappa, C. Hu, W. Yu, L. Qin, Y. Huang and H. Gao, *Adv. Funct. Mater.*, 2019, **29**, 1808462.
111 R. Liu, Y. An, W. Jia, Y. Wang, Y. Wu, Y. Zhen, J. Cao and H. Gao, *J. Controlled Release*, 2020, **321**, 589–601.
112 L. Han, X. Y. Zhang, Y. L. Wang, X. Li, X. H. Yang, M. Huang, K. Hu, L. H. Li and Y. Wei, *J. Controlled Release*, 2017, **259**, 40–52.
113 M. Ye, Y. Han, J. Tang, Y. Piao, X. Liu, Z. Zhou, J. Gao, J. Rao and Y. Shen, *Adv. Mater.*, 2017, **29**, 1702342.
114 Y. Kang, X. Ju, L. S. Ding, S. Zhang and B. J. Li, ACS Appl, *ACS Appl. Mater. Interfaces*, 2017, **9**, 4475–4484.
115 Y. Tian, M. Lei, L. Yan and F. An, *Polym. Chem.*, 2020, **11**, 2360–2369.
116 B. Z. Hailemeskel, K. D. Addisu, A. Prasannan, S. L. Mekuria, C.-Y. Kao and H.-C. Tsai, *Appl. Surf. Sci.*, 2018, **449**, 15–22.
117 N. Ma, Y. Li, H. Xu, Z. Wang and X. Zhang, *J. Am. Chem. Soc.*, 2010, **132**, 442–443.
118 L. Wang, W. Cao, Y. Yi and H. Xu, *Langmuir*, 2014, **30**, 5628–5636.
119 D. Shao, M. Li, Z. Wang, X. Zheng, Y. H. Lao, Z. Chang, F. Zhang, M. Lu, J. Yue, H. Hu, H. Yan, L. Chen, W. F. Dong and K. W. Leong, *Adv. Mater.*, 2018, **30**, 1801198.
120 D. Shao, F. Zhang, F. Chen, X. Zheng, H. Hu, C. Yang, Z. Tu, Z. Wang, Z. Chang, J. Lu, T. Li, Y. Zhang, L. Chen, K. W. Leong and W. F. Dong, *Adv. Mater.*, 2020, **32**, 2004385.
121 Y. Yang, F. Chen, N. Xu, Q. Yao, R. Wang, X. Xie, F. Zhang, Y. He, D. Shao, W. F. Dong, J. Fan, W. Sun and X. Peng, *Biomaterials*, 2022, **281**, 121368.
122 S. Pandit, D. Dutta and S. Nie, *Nat. Mater.*, 2020, **19**, 478–480.
123 S. Sindhwani, A. M. Syed, J. Ngai, B. R. Kingston, L. Maiorino, J. Rothschild, P. MacMillan, Y. Zhang, N. U. Rajesh, T. Hoang, J. L. Y. Wu, S. Wilhelm, A. Zilman, S. Gadde, A. Sulaiman, B. Ouyang, Z. Lin, L. Wang, M. Egeblad and W. C. W. Chan, *Nat. Mater.*, 2020, **19**, 566–575.
124 P. Wei and J. S. Moodera, *Nat. Mater.*, 2020, **19**, 481–482.
125 J. He, C. Li, L. Ding, Y. Huang, X. Yin, J. Zhang, J. Zhang, C. Yao, M. Liang, R. P. Pirraco, J. Chen, Q. Lu, R. Baldridge, Y. Zhang, M. Wu, R. L. Reis and Y. Wang, *Adv. Mater.*, 2019, **31**, 1902409.
126 Y. Ding, Y. Wang and Q. Hu, *Exploration*, 2022, **2**, 20210106.